SUPPLEMENTARY INFORMATION FOR:

The value of remote marine aerosol measurements for constraining radiative forcing uncertainty

Leighton A. Regayre[1], Julia Schmale[2], Jill S. Johnson[1], Christian Tatzelt[3], Andrea Baccarini[2], Silvia Henning[3], Masaru Yoshioka[1], Frank Stratmann[3], Martin Gysel-Beer[2] and Ken S. Carslaw[1]

[1]Institute for Climate and Atmospheric Science, School of Earth and Environment, University of Leeds, Leeds, LS2 9JT, UK
[2]Paul Scherrer Institute, Laboratory of Atmospheric Chemistry, Villigen, Switzerland
[3]Leibniz Institute for Tropospheric Research, Leipzig, Germany

Correspondence to: Leighton Regayre (L.A.Regayre@leeds.ac.uk)
Correspondence related to measurements to: Julia Schmale (julia.schmale@psi.ch)

SI Methods

SI Methods: Model Version

We use the Global Atmosphere 4 (GA 4.0; Walters et al., 2014) configuration of the Hadley Centre General Environment Model version 3 (HadGEM3; Hewitt et al., 2011), which incorporates the UK Chemistry and Aerosol (UKCA) model at version 8.4 of the UK Met Office's Unified Model (UM). UKCA simulates trace gas chemistry and the evolution of the aerosol particle size distribution and chemical composition using the GLObal Model of Aerosol Processes (GLOMAP-mode; Mann et al., 2010) and a whole-atmosphere chemistry scheme (Morgenstern et al., 2009; O'Connor et al., 2014). The model has a horizontal resolution of 1.25x1.875 degrees and 85 vertical level. The aerosol size distribution is defined by seven log-normal modes: one soluble nucleation mode as well as soluble and insoluble Aitken, accumulation and coarse modes. The aerosol chemical components are sulfate, sea salt, black carbon (BC), organic carbon (OC) and dust. Secondary organic aerosol (SOA) material is produced from the first stage oxidation products of biogenic monoterpenes under the assumption of zero vapour pressure and is combined with primary particulate organic matter after kinetic condensation. Use of the GLOMAP model to simulate aerosol size and composition changes reduces Southern Ocean radiative biases in HadGEM3 (Bodas-Salcedo et al., 2019).

GLOMAP simulates new particle formation, coagulation, gas-to-particle transfer, cloud processing and deposition of gases and aerosols. The activation of aerosols into cloud droplets is calculated using globally prescribed distributions of sub-grid vertical velocities (West et al. 2014) and the removal of cloud droplets by autoconversion to rain is calculated by the host model. Aerosols are also removed by impaction scavenging of falling raindrops according to the collocation of clouds and precipitation (Lebsock et al., 2013; Boutle et al., 2014). Aerosol water uptake efficiency is determined by kappa-Kohler theory (Petters and Kreidenweis, 2007) using composition-dependent hygroscopicity factors.

We prescribe anthropogenic emissions using the emission inventory prepared for the Atmospheric Chemistry and Climate Model Inter-comparison Project (ACCMIP) and also prescribed in some of the CMIP Phase 5 experiments. Present-day carbonaceous aerosol emissions were prescribed using a ten year average of 2002 to 2011 monthly mean data from the Global Fire and Emissions Database (GFED3; van der Werf et al., 2010) and according to Lamarque et al. (2010) for 1850. We prescribe volcanic SO2 emissions for continuously emitting and sporadically erupting volcanoes (Andres et al., 1998) and for explosive volcanic eruptions (Halmer et al., 2002). Surface ocean dimethyl-sulfide concentrations are prescribed using Kettle and Andreae (2000) and emitted into the atmosphere using a surface wind speed dependent parametrisation (following Nightingale et al., 2000). Sea spray is emitted into the atmosphere using the Gong (2003) surface wind speed dependent parametrisation.

Several modifications were made to version 8.4 of UKCA to overcome known structural deficiencies in the model. An organically-mediated boundary layer nucleation parametrisation (Metzger et al., 2010) was included so that remote marine and early-industrial aerosol concentrations were not unrealistically low in the model. We also added a parametrisation for ice crystal suppression of precipitation known to bring remote marine aerosol concentrations in line with measurements (Browse et al., 2012). Dust in the base model is calculated using the CLASSIC bin scheme (Woodward et al., 2001), which we replaced in our model version so that dust is emitted using the GLOMAP modal scheme. This means interactions between dust and other aerosols are explicitly simulated. We better resolve the optical properties of aerosols across wavelengths by improving the resolution of the default look-up tables. Finally, we made minor adjustments to some process parametrisations so that parameter values could be perturbed globally. All changes to the model are described fully in Yoshioka et al. (2019).

SI Methods: Perturbed Parameter Ensembles

We make use of the ATM and AER-ATM perturbed parameter ensembles (PPEs) described in Yoshioka et al. (2019). Results in the main article make use of the AER PPE except for the quantification of aerosol ERF and its components. These two PPEs were designed to provide complementary insights into causes of uncertainty in the climate system. The 235 member AER PPE samples uncertainties in a set of 26 aerosol parameters, whilst the 191 member AER-ATM PPE samples uncertainties in 18 aerosol and 9 physical atmosphere parameters related to clouds, radiation and moisture. The effects of rapid atmospheric adjustments to aerosols are not included in AER, but are included in AER-ATM (although they have a relatively minor impact on aerosol forcing in this model (Mulcahy et al., 2018). Therefore, ERF is calculated for the AER-ATM PPE and combined with the CERES top-of-the-atmosphere constraint employed in Regayre et al. (2018), whilst RF is calculated for the AER PPE and combined with the predominantly Northern Hemisphere aerosol constraint employed in Johnson et al. (2019).

Both PPEs were nudged towards European Centre for Medium-Range Weather Forecasts (ECMWF) ERA-Interim reanalyses. Nudging means that pairs of simulations have near-identical synoptic-scale features, which enables the effects of parameter perturbations to be quantified using single-year simulations, although the magnitude of forcing will vary with the chosen year (Yoshioka et al., 2019; Fiedler et al., 2019). We nudge well above the Earth's surface in order to strike a balance between the computational cost of perturbing multiple parameters and the computational saving of using prescribed meteorology to overcome internal variability (Zhang et al., 2016). In the AER-ATM PPE only horizontal winds above the boundary layer (around 2km) for the year 2006 were prescribed, whilst in AER, horizontal winds and temperatures for 2008 were prescribed above around 1km. In each PPE the model was allowed to respond to parameter perturbations (a spin-up period) prior to simulating the data used here. Despite these differences, results in the main article are consistent across the PPEs.

SI Methods: Sampling and uncertainty

We sample uncertainty in model output using uniform pdfs across each parameter range. The uncertainty in individual parameters could be sampled in a more informed manner. For example, Yoshioka et al. (2019) used expert elicited information about likely parameter values to create parameter pdfs, which were used by Watson-Paris et al. (submitted) to sample uncertainty in aerosol forcing uncertainty. The additional information provided by expert elicited parameter pdfs is invaluable for quantifying the causes of model uncertainty (e.g. Regayre et al., 2018) because the choice of pdfs affects the contributions to variance in model output. However, in nearly 30 dimensions, samples of combined parameter value using multiple pdfs with centralised tendencies will by heavily weighted towards the centre of the parameter space. Since our intention in this article is to sample the range of model behaviour in response to the full spectrum of uncertain parameter combinations prior to constraint using measurements, we use uniform pdfs with maximum and minimum values from the expert elicited ranges.

A set of around 200 model variants that make up the PPEs are much too small to allow statistical analysis of model performance across nearly 30 dimensions of parameter space. We therefore use output from the PPEs to train Gaussian Process emulators (e.g. Lee et al., 2012), which define how the model outputs vary continuously over the parameter space. Some additional uncertainty is caused by emulating (rather than simulating) model output and this uncertainty is incorporated into our model-measurement constraint process. We sample Monte Carlo points from the emulated parameter space to produce the set of one million model variants.

SI Methods: Measurements

Measurements were collected during the ACE-SPACE campaign between December 2016 and March 2017. The measurement methodology is explained in Schmale et al. (2019) as well as in the metadata of the datasets cited below. We constrain the model uncertainty using near-surface measurements of cloud condensation nuclei concentrations at 0.2% and 1.0% supersaturations ($CCN_{0.2}$ and $CCN_{1.0}$; Tatzelt et al., 2019), as well as number concentrations of particles larger than 700 nm (N_{700}; Schmale et al., 2019a) and mass concentrations of non-sea-salt sulfate in PM_{10}. We compare simulated and measured $CCN_{0.2}$ concentrations because cloud-active aerosol concentrations are fundamentally important for RF_{aci}. We use $CCN_{1.0}$ measurements to challenge the model's ability to reproduce concentrations of relatively small aerosols that only activate to form cloud droplets at very high supersaturations. We target the highly uncertain sea spray emission flux scaling parameter by comparing concentrations of N_{700} to simulated concentrations of sea spray aerosol, under the assumption that over the Southern Ocean, sea spray is the predominant (if not only) source of relatively large aerosols. Finally, we compare non sea salt sulfate concentrations (which omit primary sulfate in sea spray aerosol) in order to constrain the uncertainty in the emission flux of dimethyl-sulphide from the ocean surface. The sea salt fraction of sulfate was calculated using sodium as a tracer for the enrichment of sea salt in the aerosol phase (Sander et al., 2003). Non-sea-salt sulfate was calculated by subtracting this fraction from the total particulate sulfate as detected from PM10 filters.

Data for all variables were averaged for comparison with monthly mean model values by taking the mean of all data points that were collected at locations corresponding to positions within model gridboxes. This spatial and temporal degradation introduces representation errors that we account for using our model-measurement comparison (next section). However, the reduction in data volume makes the model-measurement comparison over one million model variants tractable.

SI Methods: Model-measurement comparisons

Our constraint approach follows Johnson et al. (2019) and involves comparing model variants (parameter combinations) to a set of measurements and ruling out variants that are judged to be implausible. This method uses the statistical methodology of history matching, which has been effectively applied to complex models in a range of fields (Craig et al., 1997; Williamson et al., 2013; McNeall et al., 2016; Rodrigues et al., 2017 and Andrianakis et al., 2017). We account for emulator uncertainty, measurement uncertainty (instrument error) and representativeness uncertainties (caused by spatial and temporal mismatches in resolution and sampling between model and measurements). We do not include potential structural errors (e.g. from missing processes) in our constraint approach because such errors cannot be robustly quantified a priori.

For each measurement we calculate a 'measure of implausibility' for each of the one million model variants, calculated as the model-measurement difference standardised by the combined emulator, measurement and representativeness uncertainties. Using this 'implausibility measure' we can identify implausible model variants and rule our implausible parts of parameter space via the combination of the 'closeness' of the measurement and model output, and the size of the related uncertainties.The 'implausibility metric' is as:

$$I(\boldsymbol{x}) = \frac{|\, M - O \,|}{\sqrt{[Var(M) + Var(O) + Var(R)]}}, \quad (1)$$

where *M* is the model variant output and *O* is the observed value (the measurement). In the denominator *Var(M)* is the variance in the model estimate (caused by emulator uncertainty), *Var(O)* is the variance in the measurement (i.e., instrument or retrieval uncertainty) and the representativeness error, *Var(R)*, is the variance associated with comparing model output to measurements at different spatial (Schutgens et al., 2016a; Weigum et al. 2016, Schutgens et al., 2017) and temporal (Schutgens et al., 2016b; Schutgens et al., 2017) resolutions. We compare the 2016-17 measurements to the models nudged towards 2008 meteorology for AER and 2008 meteorology for AER-ATM because the measurements were not collected when the PPE was created. The *Var(R)* term therefore includes additional uncertainty due to inter-annual variability. According to the definition of the implausibility measure, model variants will not be ruled out if either the model-measurement difference is small or the uncertainty in the denominator is large. In other words, we retain model variants that are skilful and

model variants whose skill cannot be adequately determined because the model-measurement comparison uncertainties are too large.

The variance terms in the denominator of Eq. (1) are calculated uniquely for each measurement. Following Johnson et al., (2019), we use a measurement uncertainty of 10%, a spatial co-location uncertainty of 20% and a temporal co-location uncertainty of 20%. Emulator uncertainty is calculated for each model-measurement combination using the error on the predicted mean from the emulator for the model variant. We use residuals in de-trended monthly mean output from a HadGEM-UKCA hindcast simulation over the period of 1980-2009 (Turnock et al., 2015) to estimate the inter-annual variability for each variable across all model gridboxes and months.

We calculate implausibility values for each of the one million model variants for every measurement. Deciding which model variants to retain would be trivial were we comparing the sample output to a single measurement. We would sequentially rule out the variant with the highest implausibility metric until some small fraction of the original sample remained. However, our task is more complex. We need to rule out model variants based on multiple implausibility metrics that are distinct for each measurement location and measurement type.

A variant may compare well with a measurement type in one location and poorly in another because spatial and temporal features in the measurement data (e.g. changing aerosol sources) mean each measurement could provide different information about the plausibility of the models. To avoid prematurely ruling out model variants based on a few poor comparisons, we only rule out variants if their implausibility exceeds a defined threshold for more than a tolerable fraction of measurements. We choose threshold and tolerance values with a goal of retaining around 3% of the original sample. The subjective choice of 3% retention determines the results to some extent. Retaining a smaller percentage of the model variants could potentially over-constrain the model. However, retaining a larger proportion risks weakening the constraint and retaining addition implausible variants.

SI Results

SI Results: Constrained marginal parameter distributions

In Fig. 3 of the main article we show the marginal probability distributions for the 26 parameters in the AER PPE. These marginal distributions show the effect of measurement constraint on individual parameter likelihoods. Rejecting the majority of the model variants reduces the maximum density, so marginal densities for the constrained sample are scaled such that the tops of the constrained and unconstrained pdfs are aligned. Similar parameter constraints are found when constraining the AER-ATM PPE using the same constraint process and original set of measurements (Fig. S1). In addition to parameters that are perturbed in both PPEs, we show the effect of measurement constraint on the few physical atmosphere parameters (Rad_Mcica_Sigma and Fac_Qsat) that are constrained by our process as well as additional aerosol parameters that were perturbed in AER-ATM (BC_RI and OC_RI).

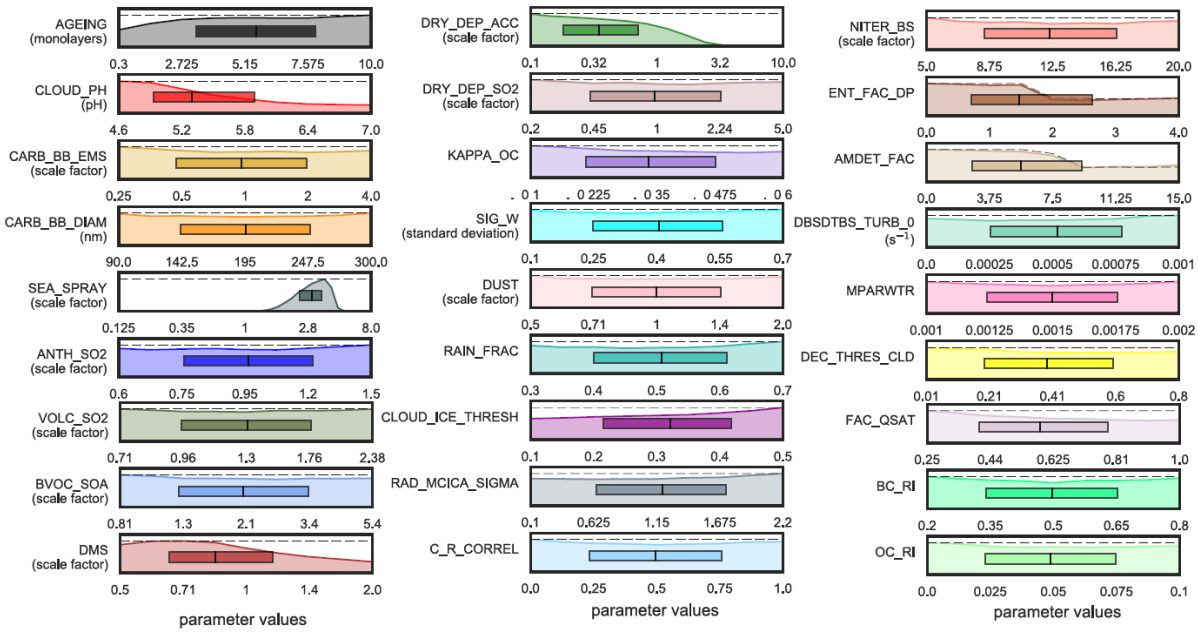

Fig. S1. Marginal probability distributions for aerosol and physical atmosphere parameters from the AER-ATM PPE after constraint. The density of parameter values in the unconstrained sample are shown as dashed lines. Densities of constrained samples are shown in colour. The 25th, 50th and 75th percentiles of each marginal distribution are shown in the central boxes. Parameter values on the x-axes correspond to values used in the model (Yoshioka et al., 2019).

SI Results: Wind Speed discrepancies

Southern Ocean wind speeds during the ACE-SPACE expedition were often much lower than climatological mean values, but on average were higher than winds in our ensemble (Schmale et al., 2019). Wind speed discrepancies do not affect our results, possibly because differences in the resulting wave heights cause compensating effects between sea spray emission fluxes and the removal rate of aerosols by the ocean (Korhonnen et al., 2010). Marginal parameter distributions are constrained consistently when we remove measurements with average wind speed differences larger than 50% of the measured value from the model-measurement comparison.

SI Results: Additional constraint to achieve radiative balance

We additionally test the effect of ruling out model variants that differ from the Clouds and the Earth's Radiant Energy System (CERES; Loeb et al., 2009) measurement of global, annual mean top-of-the-atmosphere outgoing shortwave radiative flux of 98.3 98.3 W m^{-2} by more than 0.25 W m^{-2}, which was the constraint used in Regayre et al., (2018). The constraint on ERF using the CERES-derived top-of-the-atmosphere fluxes in addition to the ACE-SPACE measurement dataset weakens the reduction in aerosol ERF from 8% to 7%. Fig. S2 (for comparison with Fig. 4a) shows the effect of this additional constraint on aerosol ERF. Retaining only model variants that agree with top-of-the-atmosphere radiative flux measurements does not noticeably affect the constraint on aerosol ERF (as shown in Regayre et al., 2018). Furthermore, the marginal parameter pdfs are unaffected by the additional constraint.

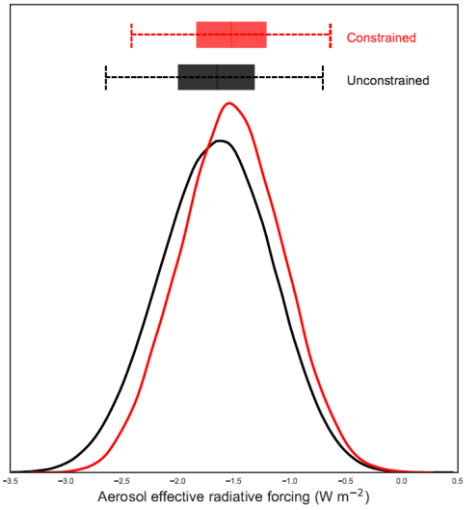

Fig. S2. Probability distribution of ERF_{aci} from the AER-ATM PPE. Values from the unconstrained sample of one million model variants are in black. Red lines show the values constrained by ACE-SPACE measurements and additionally constrained using CERES top-of-the-atmosphere measurements. Plotting features are identical to Fig. 4.

SI References:

Adrianakis, I., Vernon, I., McCreesh, N., McKinley, T. J., Oakley, J. E., Nsubuga, R. N., Goldstein, M., and White, R. G.: History matching of a complex epidemiological model of human immunodeficiency virus transmission by using variance emulation, J. Roy. Stat. Soc. C-App., 66, 717–740, doi:10.1111/rssc.12198, 2017.

Andreae, M. O., Jones, C. D., and Cox, P. M.: Strong present-day aerosol cooling implies a hot future, Nat., 435, 1187–1190, doi:10.1038/nature03671, 2005.

Andres, R. J. and Kasgnok, A. D.: A time-averaged inventory of subaerial volcanic sulfur emissions, J. Geo. Res., 103, 25 251–25 262, doi:10.1029/98JD02091, 1998.

Bodas-Salcedo, A., Mulcahy, J. P., Andrews, T., Williams, K. D., Ringer, M. A., Field, P. R., and Elsaesser, G. S.: Strong dependence of atmospheric feedbacks on mixed-phase microphysics and aerosol-cloud interactions in HadGEM3, J. Adv. Model. Earth Syst., 11, 1735–1758, doi:10.1029/2019MS001688, 2019.

Boutle, I. A., Abel, S. J., Hill, P. G., and Morcrette, C. J.: Spatial variability of liquid cloud and rain: observations and microphysical effects, Quart. J. Roy. Meteor. Soc., 140, 585–594, doi:10.1002/qj.2140, 2014.

Browse, J., Carslaw, K. S., Arnold, S. R., Pringle, K. J., and Boucher, O.: The scavenging processes controlling the seasonal cycle in Arctic sulphate and black carbon aerosol, Atmos. Chem. Phys., 12, 6775–6798, doi:10.5194/acp-12-6775-2012, 2012.

Carslaw, K. S., Boucher, O., Spracklen, D. V., Mann, G. W., Rae, J. G. L., Woodward, S., and Kulmala, M.: A review of natural aerosol interactions and feedbacks within the Earth system, Atmos. Chem. Phys., 10, 1701–1737, 10.5194/acp-10-1701-2010, 2010.

Carslaw, K. S., Lee, L. A., Reddington, C. L., Pringle, K. J., Rap, A., Forster, P.M.,Mann, G.W., Spracklen, D. V.,Woodhouse,M., Regayre, L. A., and Pierce, J. R.: Large contribution of natural aerosols to uncertainty in indirect forcing, Nat., 503, 67–71, doi:10.1038/nature12674, 2013.

Carslaw, K. S., Gordon, H., Hamilton, D. S., Johnson, J. S., Regayre, L. A., and Yoshioka, M.: Aerosols in the pre-industrial atmosphere, Curr. Clim. Change Rep., 3, 1–15, doi:10.101007/s40641-017-0061-2, 2017.

Collins, M., Knutti, R., Arblaster, J., Dufresne, J. L., Fichefet, D., Friedlingstein, P., Gao, X., Gutowski, W. J., Johns, T., Krinner, G., Shongwe, M., Tebaldi, C., Weaver, A. J., and Wehner, M.: Long-term Climate Change: Projections Commitments and Irreversibility, in: Climate Change 2013: The Physical Science Basis. Contribution of Working Group I to the Fifth Assessment Report of the Intergovernmental Panel on Climate Change, edited by Stocker, T. F., Qin, D., Plattner, G. K., Tignor, M., Allen, S. K., Boschung, J., Nauels, A., Xia, Y., Bex, V., and Midgley, P. M., Cambridge University Press, Cambridge, United Kingdom and New York, NY, USA, 2013.

Craig, P. S., Goldstein,M., Seheult, A. H., and Smith, J. A.: Pressure Matching for Hydrocarbon Reservoirs: A Case Study in the Use of Bayes Linear Strategies for Large Computer Experiments, in: Case Studies in Bayesian Statistics. Lecture Notes in Statistics, edited by Gatsonis, C., Hodges, J. S., Kass, R. E., McCulloch, R., Rossi, P., and N.D., N. D. S., Springer, New York, NY, doi:10.1007/978-1-4612-2290-3_2, 1997.

Fiedler, S., Kinne, S., Katty Huang, W. T., Räisänen, P., O'Donnell, D., Bellouin, N., Stier, P., Merikanto, J., van Noije, T., Carslaw, K. S., Makkonen, R., and Lohman, U.: Anthropogenic aerosol forcing – insights from multi-estimates from aerosol-climate models with reduced complexity, Atmos. Chem. Phys., 19, TBA, doi:10.5194/acp-2018-639, 2019.

Gong, S. L.: A parameterization of sea-salt aerosol source function for sub- and super-micron particles, Glob. Biogeochem. Cyc., 17, 1097, doi:10.1029/2003GB002079, 2003.

Gryspeerdt, E., Quaas, J., Ferrachat, S., Gettelman, A., Ghan, S., Lohmann, U., Morrison, H., Neubauer, D., Partridge, D. G., Stier, P., Takemura, T., Wang, H., Wang, M., and Zhang, K.: Constraining the instantaneous aerosol influence on cloud albedo, Proc. Natl. Acad. Sci., 114, 4899–4904, doi:10.1073/pnas.1617765114, 2017.

Halmer, M., Schmincke, H. U., and Graf, H. F.: The annual volcanic gas input into the atmosphere, in particular into the stratosphere: a global data-set for the past 100 years, J. Volcanol. Geotherm. Res., 115, 511–528, doi:10.1016/S0377-0273(01)00318-3, 2002.

Hamilton, D. S., Lee, L. A., Pringle, K. J., Reddington, C. L. S., Spracklen, D. V., and Carslaw, K. S.: Occurrence of pristine aerosol on a polluted planet, Proc. Natl. Acad. Sci., 111, 18 466–18 471, doi:10.1073/pnas.1415440111, 2014.

Hewitt, H. T., Copsey, D., Culverwell, I. D., Harris, C. M., Hill, R. S. R., Keen, A. B., McLaren, A. J., and Hunke, E. C.: Design and implementation of the infrastructure of HadGEM3: the next-generation Met Office climate modelling system, Geosci. Mod. Dev., 4, 223–253, doi:10.5194/gmd-4-223-2011, 2011.

Johnson, J. S., Regayre, L. A., Yoshioka, M., Pringle, K. J., Turnock, S. T., Browse, J., and Carslaw, K. S.: Robust observational constraint of processes and emissions in a climate model and the effect on aerosol radiative forcing, Atmos. Chem. Phys. Discuss., doi:10.5194/acp-2019-834, in review, 2019.

Kelle, A. J. and Andreae, M. O.: Flux of dimethylsulphide from the oceans: A comparison of updated data sets and flux models, J. Geo. Res. Atmos., 105, 26 793–26 808, doi:10.1029/2000JD900252, 2000.

Korhonen, H., Carslaw, K. S., Forster, P., Mikkonen, S., Gordon, N. D., and Kokkola, H.: Aerosol climate feedback due to decadal increases in Southern Hemisphere wind speeds, Geophys. Res. Lett., 37, L02805-6, doi:10.1029/2009GL041320, 2010.

Lamarque, J. F., Bond, T. C., Eyring, V., Granier, C., Heli, A., Kilmont, Z., Lee, D., Liousse, C., Mieville, A., Owen, B., Schultz, M. G., Shindell, D., Smith, S. J., Stehfest, E., Van Aardenne, J., Cooper, O. R., Kainuma, M., Mahowald, N., McConnell, J. R., Naik, V., Riahi, K., and van Vuuren, D. P.: Historical (1850-2000) gridded anthropogenic and biomass burning emissions of reactive gases and aerosols: methodology and application, Atmos. Chem. Phys., 10, 7017–7039, doi:10.5194/acp-10-7017-2010, 2010.

Lebsock, M., Morrison, H., and Gettleman, A.: Mircophysical implications of cloud-precipitation covariance derived from satellite remote sensing, J. Geo. Res. Atmos., 118, 6521–6533, doi:10.1001/jgrd.50347, 2013.

Lee, L. A., Carslaw, K. S., Pringle, K. J., and Mann, G. W.: Mapping the uncertainty in global CCN using emulation, Atmos. Chem. Phys., 12, 9739–9751, doi:10.5194/acp-12-9739-2012, 2012.

Lee, L. A., Reddington, C. L., and Carslaw, K. S.: On the relationship between aerosol model uncertainty and radiative forcing uncertainty, Proc. Natl. Acad. Sci., 113, 5820–5827, doi:10.1073/pnas.1507050113, 2016.

Loeb, N. G.,Wielicki, B. A., Doelling, D. R., Smith, G. L., Keyes, D. F., Kato, S., Manalo-Smith, N., and Wong, T.: Toward Optimal Closure of the Earth's Top-of-Atmosphere Radiation Budget, J. Climate., 22, 748–766, doi:10.1175/2008JCLI2637.1, 2009.

Mann, G. W., Carslaw, K. S., Spracklen, D. V., Ridley, D. A., Manktelow, P. T., Chipperfield, M. P., Pickering, S. J., and Johnson, C. E.: Description and evaluation of GLOMAP-mode aerosol microphysics model for the UKCA composition-climate model, Geosci. Mod. Dev., 3, 519–551, doi:10.5194/gmd-3-519-2010, 2010.

McCoy, D. T., Bender, F. A., Mohrmann, J. K. C., Hartmann, D. L., Wood, R., and Grosvenor, D. P.: The global aerosol-cloud first indirect effect estimated using MODIS, MERRA, and AeroCom, JGRA, 122, 1779–1796, doi:10.1002/2016JD026141, 2017.

McNeall, D., Williams, J., Booth, B. B. B., Betts, R., Challenor, P., Wiltshire, A., and D.Sexton: The impact of structural error on parameter constraint in a climate model, Ear. Sys. Dyn., 7, 917–935, doi:10.5194/esd-7-917-2016, 2016.

Metzger, A., Verheggen, B., Dommen, J., Duplissy, J., Prevot, A. S. H.,Weingartner, E., Riipinen, I., Kulmala, M., Spracklen, D. V., Carslaw, K. S., and Baltensperger, U.: Evidence for the role of organics in aerosol particle formation under atmospheric conditions, Proc. Natl. Acad. Sci., 107, 6646–6651, doi:10.1073/pnas.0911330107, 2010.

Morgenstern, O., Braesicke, P., O'Connor, F. M., Bushell, A. C., Johnson, C. E., Osprey, S. M., and Pyle, J. A.: Evaluation of the new UKCA climate-composition model – Part 1: The stratosphere, Geosci. Mod. Dev., 2, 43–57, doi:10.5194/gmd-2-43-2009, 2009.

Mulcahy, J., Jones, C., Sellar, A., Johnson, B., Boutle, I. A., Jones, A., Andrews, T., Rumbold, S. T., Mollard, J., Bellouin, N., Johnson, C. E., Williams, K. D., Grosvenor, D. P., and McCoy, D. T.: Improved aerosol processes and effective radiative forcing in HadGEM3 and UKESM1, J. Adv. Model. Earth Syst., 10, 2786—2805, doi:10.1029/2018MS001464, 2018.

Myhre, G., Shindell, D., Bréon, F. M., Collins, W., Fuglestvedt, J., Huang, J., Koch, D., Lamarque, J. F., Lee, D., Mendoza, B., Nakajima, T., Robock, A., Stephens, G., Takemura, T., and Zhang, H.: Anthropogenic and Natural Radiative Forcing, in: Climate Change 2013: The Physical Science Basis. Contribution of Working Group I to the Fifth Assessment Report of the Intergovernmental Panel on Climate Change, edited by Stocker, T. F., Qin, D., Plattner, G. K., Tignor, M., Allen, S. K., Boschung, J., Nauels, A., Xia, Y., Bex, V., and Midgley, P. M., Cambridge University Press, Cambridge, United Kingdom and New York, NY, USA, 2013.

Nightingale, P. D., Liss, P. S., and Schlosser, P.: Measurements of air-sea gas transfer during an open ocean algal bloom, Geophys. Res. Lett., 27, 2117–2120, doi:10.1029/2000GL011541, 2000.

O'Connor, F. M., Johnson, C. E., Morgenstern, O., Abraham, N. L., Braesicke, P., Dalvi, M., Folberth, G. A., Sanderson, M. G., Telford, P. J., Voulgarakis, A., Young, P. J., Zeng, G., Collins,W. J., and Pyle, J. A.: Evaluation of the new UKCA climate-composition model-Part 2: The troposphere, Geosci. Mod. Dev., 7, doi:10.5194/gmd-7-41-2014, 2014.

Petters, M. D. and Kreidenweis, S. M.: A single parameter representation of hygroscopic growth and cloud condensation nucleus activity, Atmos. Chem. Phys., 7, 1961–1971, doi:10.5194/acp-7-1961-2007, 2007.

Regayre, L. A., Pringle, K. J., Booth, B. B. B., Lee, L. A., Mann, G. W., Browse, J., Woodhouse, M. T., Rap, A., Reddington, C. L. S., and Carslaw, K. S.: Uncertainty in the magnitude of aerosol-cloud radiative forcing over recent decades, Geophys. Res. Lett., 41, 9040–9049, doi:10.1002/2014GL062029, 2014.

Regayre, L. A., Johnson, J. S., Yoshioka, M., Pringle, K. J., H.Sexton, D. M., Booth, B. B. B., Lee, L. A., Bellouin. N., and Carslaw, K. S.: Aerosols and physical atmosphere model parameters are both important sources of uncertainty in aerosol ERF, ACP, 18, 9975–10 006, doi:10.5194/acp-18-9975-2018, 2018.

Rodrigues, L. F. S., Vernon, I., and Bower, R.: Constraints on galaxy formation models from the galaxy stellar mass function and its evolution, Mon. Not. R. Astron. Soc., 466, 2418–2435, doi:10.1093/mnras/stw3269, 2017.

Sander, R., Keene, W. C., Pszenny, A. A. P., Arimoto, R., Ayers, G. P., Baboukas, E., Cainey, J. M., Crutzen, P. J., Duce, R. A., Hönninger, G., Huebert, B. J., Maenhaut, W., Mihalopoulos, N., Turekian, V. C., and Van Dingenen, R.: Inorganic bromine in the marine boundary layer: a critical review, Atmos. Chem. Phys., 3, 1301–1336, doi:10.5194/acp-3-1301-2003, 2003.

Schmale, J., Baccarini, A., Thurnherr, I., Henning, S., Efraim, A., Regayre, L. A., Bolas, C., Hartmann, M.,Welti, A., Lehtipalo, K., Aemisegger, F., Tatzelt, C., Landwehr, S., Modini, R., Tummon, F., Johnson, J. S., Harris, N., Schnaiter, M., Toffoli, A., Derkani, M., Bukowiecki, N., Stratmann, F., Dommen, J., Baltensperger, U., Wernli, H., Rosenfeld, D., Gysel-Beer, M., and Carslaw, K.: Overview of the Antarctic Circumnavigation Expedition: Study of Preindustrial-like Aerosols and Their Climate Effects (ACE-SPACE), Bull. Amer. Meteorol. Soc., Early Online Release, doi:10.1175/BAMS-D-18-0187.1, 2019.

Schmale, J., Henning, S., Tummon, F., Hartmann, M., Baccarini, A., Welti, A., Lehtipalo, K., Tatzelt, C., Landwehr, S. and Gysel-Beer, M.: Course mode aerosol particle size distribution collected in the Southern Ocean in the austral summer of 2016/2017, during the Antarctic Circumnavigation Expedition, Version 1.0 Dataset, doi:10.5281/zenodo.2636709, 2019a.

Schutgens, N., Gryspeerdt, E., Weigum, N., Tsyro, S., Goto, D., Schulz, M., and Stier, P.: Will a perfect model agree with perfect observations? The impact of spatial sampling, Atmos. Chem. Phys., 16, 6335–6353, doi:10.5194/acp-16-6335-2016, 2016a.

Schutgens, N., Partridge, D., and Stier, P.: The importance of temporal collocation for the evaluation of aerosol models with observations, Atmos. Chem. Phys., 16, 1065–1079, doi:10.5194/acp-16-1065-2016, 2016b.

Schutgens, N., Tsyro, S., Gryspeerdt, E., Goto, D., Weigum, N., Schulz, M., and Stier, P.: On the spatio-temporal representativeness of observations, Atmos. Chem. Phys., 17, 9761–9780, doi:10.5194/acp-17-9761-2017, 2017.

Seinfeld, J. H., Bretherton, C., Carslaw, K. S., Coe, H., DeMott, P. J., Dunlea, E. J., Feingold, G., Ghan, S., Guenther, A. B., Kahn, R., Kraucunas, I., Kreidenweis, S. M., Molina, M. J., Nenes, A., Penner, J. E., Prather, K. A., Ramanathan, V., Ramaswamy, V., Rasch, P. J., Ravishankara, A. R., Rosenfeld, D., Stephens, G., and Wood, R.: Improving our fundamental understanding of the role of aerosol-cloud interactions in the climate system, Proc. Natl. Acad. Sci., 113, 5781–5790, doi:10.1073/pnas.1514043113, 2016.

Spracklen, D. V. and Rap, A.: Natural aerosol-climate feedbacks suppressed by anthropogenic aerosol, Geophys. Res. Lett., 40, 5316–5319, doi:10.1002/2013GL057966, 2013.

Stocker, T. F., Qin, D., Plattner, G. K., Tignor, M., Allen, S. K., Boschung, J., Nauels, A., Xia, Y., Bex, V., and Midgley, P. M.: Summary for Policymakers, in: Climate Change 2013: The Physical Science Basis. Contribution of Working Group I to the Fifth Assessment Report of the Intergovernmental Panel on Climate Change, edited by Stocker, T. F., Qin, D., Plattner, G. K., Tignor, M., Allen, S. K., Boschung, J., Nauels, A., Xia, Y., Bex, V., and Midgley, P. M., Cambridge University Press, Cambridge, United Kingdom and New York, NY, USA, 2013.

Tatzelt, C., Henning, S., Tummon, F., Hartmann, M., Baccarini, A., Welti, A., Lehtipalo, K. and Schmale, J.: Cloud Condensation Nuclei number concentrations over the Southern Ocean during the austral summer of 2016/2017, Version 1.0 Data set, doi:10.5281/zenodo.2636765, 2019.

Tett, S. F. B., Rowlands, D. J., Mineter, M. J., and Cartis, C.: Can Top-Of-Atmosphere Radiation Measurements Constrain Climate Predictions? Part II: Climate Sensitivity, J. Climate., 26, 9367–9383, doi:10.1175/JCLI-D-12-00596.1, 2013.

Turnock, S. T., Spracklen, D. V., Carslaw, K. S., Mann, G. W., Woodhouse, M. T., Forster, P. M., Haywood, J., Johnson, C. E., Dalvi, M., Bellouin, N., and Sanchez-Lorenzo, A.: Modelled and observed changes in aerosols and surface solar radiation over Europe between 1960 and 2009, Atmos. Chem. Phys., 15, 13 457—-13 513, doi:10.5194/acpd-15-13457-2015, 2015.

van der Werf, G. R., Randerson, J. T., Giglio, L., Collatz, G. J., Mu, M., Kasibhatla, P. S., Norton, D. C., DeFries, R. S., Jin, Y., and van Leeuwen, T. T.: Global fire emissions and the contribution of deforestation, savanna, forest, agricultural, and peat fires (1997-2009), Atmos. Chem. Phys., 10, 11 707–11 735, doi:10.5194/acp-10-11707-2010, 2010.

Walters, D. N., Williams, K. D., Boutle, I. A., Bushell, A. C., Edwards, J. M., Field, P. R., Lock, A. P., Morcrette, C. J., Stratton, R. A., Wilkinson, J. M., Willett, M. R., Bellouin, N., Bodas-Solcedo, A., Brooks, M. E., Copsey, D., Earnshaw, P. D., Hardiman, S. C., Harris, C. M., Levine, R. C., MacLachlan, C., Manners, J. C., Matin, G. M., Milton, S. F., Palmer, M. D., Roberts, M. J., Rosriguez, J. M., Tennant, W. J., and Vidale, P. L.: The Met Office Unified Model Global Atmosphere 4.0 and JULES Global Land 4.0 configurations, Geosci. Mod. Dev., 7, 361–386, doi:10.5194/gmd-7-361-2014, 2014.

Watson-Paris, D., Bellouin, N., Deaconu, L., Schutgens, N., Yoshioka, M., Regayre, L.A., Pringle, K.J., Johnson, J.S., Carslaw, K.S. and Stier, P.:Constraining uncertainty in aerosol direct forcing, Geophys. Res. Lett., submitted, 2019.

Weigum, N., Schutgens, N., and Stier, P.: Effect of aerosol subgrid variability on aerosol optical depth and cloud condensation nuclei: implications for global aerosol modelling, Atmos. Chem. Phys., 16, 13 619–13 639, doi:10.5194/acp-16-13619-2016, 2016.

West, R. E. L., Stier, P., Jones, A., Johnson, C. E., Mann, G. W., Bellouin, N., Partridge, D. G., and Kipling, Z.: The importance of vertical velocity variability for estimates of the indircet aerosol effects, Atmos. Chem. Phys., 14, 6369–6393, doi:10.5194/acp-14-6369-2014, 2014.

Wilcox, L. J., Highwood, E. J., Booth, B. B. B., and Carslaw, K. S.: Quantifying sources of inter-model diversity in the cloud albedo effect, Geophys. Res. Lett., 42, 1568–1575, doi:10.1002/2015GL063301, 2015.

Williamson, D., Goldstein, M., Allison, L., Blaker, A., Challenor, P., Jackson, L., and Yamazaki, K.: History matching for exploring and reducing climate model parameter space using observations and a large perturbed physics ensemble, Clim. Dyn., 41, 1703–1729, doi:10.1007/s00382-013-1896-4, 2013.

Woodward, S.: Modeling the atmospheric life cycle and radiative impact of mineral dust in the Hadley Centre climate model, J. Geo. Res., 106, 18 155–18 166, doi:10.1029/2000JD900795, 2001.

Yoshioka, M., Regayre, L. A., Pringle, K. J., Johnson, J. S., Mann, G. W., Partridge, D., Stier, P., Kipling, Z., Bellouin, N., Sexton, D. M. H ., Lister, G. M. S., Browse, J., Booth, B. B. B., Johnson, C. E., Johnson, B., Mollard, J. D. P., and Carslaw, K. S.: Ensembles of global climate model variants for the quantification and constraint of uncertainty in aerosols and their radiative forcing, J. Adv. Model. Earth Syst., Early Online Release, doi:10.1029/2019MS001628, 2019.

Zhang, S., Wang, M., Ghan, S., Ding, A., Wang, H., Zhang, K., Neubauer, D., Lohmann, U., Ferrachat, S., Takeamura, T., Gettleman, A., Morrison, H., Lee, Y. H., Shindell, D. T., Partridge, D. G., Stier, P., Kipling, Z., and Fu, C.: On the characteristics of aerosol indirect effect based on dynamic regimes in climate models, Atmos. Chem. Phys., 16, 2765–2783, doi:10.5194/acp-16-2765-2016, 2016.